SCHOOL OF ADVANCED STUDIES OF THE ROMANIAN ACADEMY

DOCTORAL SCHOOL OF CHEMICAL SCIENCES

INSTITUTE OF MACROMOLECULAR CHEMISTRY „PETRU PONI”

CHEMISTRY field

NEW FUNCTIONAL ORGANOSILICON COMPOUNDS

PhD THESIS SUMMARY

Scientific Coordinator:

Dr. MARIA CAZACU

PhD Student:

GEORGIANA-OANA ȚURCAN-TROFIN

2025

ROMANIAN ACADEMY

„Petru Poni" Institute of Macromolecular Chemestry, Iași

Mrs./Mr. .....

We inform you that on **24th of October 2025**, **12^{00}**, in **Conference Hall of the „Petru Poni" Institute of Macromolecular Chemestry, Iași**, will take place the public presentation of the doctoral thesis „***New Functional Organosilicon Compounds*** ", author **Georgiana-Oana Țurcan-Trofin**, in order to confer the scientific title of doctor.

The doctoral committee has the following composition:

PRESIDENT: **CS I Dr. Valeria Harabagiu**

„Petru Poni" Institute of Macromolecular Chemistry, Iaşi

DOCTORAL SUPERVISOR:

CS I Dr. Maria Cazacu

„Petru Poni" Institute of Macromolecular Chemistry, Iaşi

REFEREES: **Prof. Dr. Doina Humelnicu**

„Alexandru Ioan Cuza" University of Iaşi, Faculty of Chemistry

Prof. Dr. Habil.ing. Adrian Ungureanu

„Gheorghe Asachi" Technical University of Iaşi, Faculty of Chemical Engineering and Environmental Protection

CSI Dr. Corneliu Cojocaru

„Petru Poni" Institute of Macromolecular Chemistry, Iaşi

In accordance with the Regulations on the organization and PhD defense within the Romanian Academy, we send you the summary of the doctoral thesis with the kind request to communicate your appreciations and observations. On this occasion, we invite you to participate in the public defense of the doctoral thesis.

Acknowledgements

The journey to completing this thesis has been long and full of challenges, but reaching this moment brings me deep personal satisfaction. It has been a process of growth both academically and personally, and the result reflects not only my own efforts but also the support I received from those around me.

I express my deepest gratitude to my ***PhD supervisor, Dr. Maria Cazacu****, for her unconditional support and the patience with which she has guided me throughout all these years. I have always appreciated her passion for research, her openness, and the generosity with which she shared her vast experience. The knowledge, perspectives, and encouragement she provided played a vital role in my professional development and in the completion of this thesis. Above all, I am grateful to her for having the ability and openness to turn the impossible into possible at a time when I could only see limits.*

I extend my sincere thanks to ***the members of the thesis review and public defense committee*** *for their time, dedication, and for the valuable suggestions and recommendations they provided.*

Warm thanks to the members of the advisory committee, ***Prof. habil. Dr. Eng. Gabriela Lisa, Dr. Mihaela Dascălu****, and* ***Dr. Mirela Fernanda Zaltariov****, for their time, insightful comments, and helpful advice.*

I would also like to express my heartfelt thanks to all my colleagues from ***Laboratory 62****, who welcomed me with open arms and transformed a research environment into a place where I truly felt at home. It was more than just work — it was about conversations, shared laughter, daily rituals, and a team that will always hold a special place in my heart. At the same time, I am deeply grateful for for their continuous professional support: their expertise, valuable advice, and the practical help they offered whenever I needed it. I have learned from each of them, and I consider myself fortunate to have been part of such a generous and dedicated group.*

I am especially thankful to ***Dr. Mihaela Dascălu*** *for always making time to listen patiently and be there for me, offering the warmest and often the most amusing perspective, just when I needed them most. I am also grateful to* ***Dr. Mirela-Fernanda Zaltariov*** *for the knowledge she shared, for the enthusiasm and energy with which she supported every step of my work, and, not least, for her constant encouragement throughout my doctoral journey.*

*I would like to extend my sincere thanks to the **Romanian Academy** and the **"Petru Poni" Institute of Macromolecular Chemistry in Iași** for the opportunity to pursue my doctoral studies within the **Romanian Academy's School of Advanced Studies (SCOSAAR)**. I am grateful for the financial support provided, as well as for the excellent working conditions, access to research infrastructure, and the scientific expertise made available by the entire team..*

*On a personal note, I want to thank my husband, **Mihai**, for his unconditional love and support, my children, **Alexandru** and **Mara**, whose joyful and courageous outlook on the world has been an invaluable source of inspiration and strength for me — and, last but not least, my **parents** for their love and trust.*

Although this chapter is coming to an end, I carry with me gratitude for every person, every day, and every lesson.

Thank you all!

TABLE OF CONTENTS

INTRODUCTION

Since their discovery in 1934 by the American chemist James Hyde from Corning Glass Works, and named ten years later by Frederic Stanley Kipping, ***silicones*** have undergone significant evolution. Their 90-year history has been marked by various discoveries of processes and products with new properties and functionalities. In recent decades, interest in silicon-based materials has significantly increased, driven by the expansion of their applications in fields such as *biomedicine, catalysis, optoelectronics, environmental protection, and the advanced materials industry*. The evolution from crystalline silicon used in traditional semiconductors to silicon polymers, organosilicon compounds, and hybrid materials with various functionalities outlines a major direction in current research. Generally, organic-inorganic polymers that contain a polymeric backbone formed by repeating –{Si–O–} units with organic groups attached to the silicon atoms, as well as the materials derived from them, fall under the category of *silicones*. Meanwhile, compounds (either macro- or micromolecular) that contain a Si–C bond are considered *organosilicon compounds*. As such, both organosiloxane polymers and small molecules containing one or more silane or siloxane units coupled with organic groups—such as those reported in this thesis—are classified as *organosilicon compounds* (organosilicones). Depending on their nature, the attached organic groups provide specific functionalities (*biological activity, metal ion retention, catalytic activity, etc.*), which are enhanced by the coexistence of the silicon-based structural motif.

Silicon compounds/materials are synthetic derivatives of silicon, the second most abundant element in the Earth's crust. Their structure is based on silicon covalently *bonded to oxygen* and other elements, such as *carbon, hydrogen, halogens, or functional organic groups*. ***The Si–C bond*** does not occur in nature, where silicon is generally found in the form of oxygen-containing compounds (*silicates*), with which it most readily forms bonds.The basic raw material for their production is sand, which is metallurgically converted into metallic silicon. This is then subjected to the direct synthesis process (*Rochow-Müller*), which yields chlorosilanes (e.g., Me_2SiCl_2, Me_3SiCl, $MeHSiCl_2$). These are the monomers used to obtain siloxane oligomers and polymers through a hydrolysis-condensation process, forming *Si–O bonds* and releasing HCl. Thus, although the monomers are highly functionalized, in the resulting polymers the proportion of functional groups is significantly reduced, and can even reach zero, as in the case of α,ω-

bis(trimethylsiloxy)polydimethylsiloxane. This, combined with the unique characteristics of the *Si–O–Si and Si–C bonds*, gives polydiorganosiloxanes high chemical and thermal stability, as well as biological inertness, resistance to water and vapors, biocompatibility, and mechanical and electrical strength—properties required in many applications. On the other hand, the functionalization of organosiloxane compounds by attaching functional groups can significantly expand their property range and fields of application, thanks to synergistic effects between the intrinsic characteristics of the silicon-containing fragment and those of the organofunctional component.

The main objective of this thesis is the design, synthesis, and characterization of new functionalized siloxane and silane compounds, as well as the evaluation of their properties and application potential, primarily in metal ion retention and biological applications, as well as for the development of new materials (surfactants, catalysts, advanced hybrid materials).

The chosen topic aligns with current research trends focused on the *development of organic–inorganic hybrid compounds and materials* for applications in key scientific and technological fields such as *medicinal chemistry, coordination chemistry, catalysis, and materials science.* The novelty lies primarily in the synthesis of original compounds in which *chemically stable, nonpolar, and hydrophobic siloxane or silane fragments* are combined with *polar and reactive organic fragments* via *thiol–alkylation* and *thiol–ene addition reactions*—the latter being regarded as *"click" reactions*. Although the field of functionalized organosilicon compounds is rapidly evolving and the scientific literature is expanding accordingly, the contributions presented in this thesis stand out through the ***originality of the approaches***—from the selection of precursors and coupling methods to the resulting structures, the highlighted properties, and the demonstrated application potential, all validated through appropriate techniques. The research contributes to a deeper understanding of the structure–property relationships in such systems. The integration of these structures into metal complexes and metal–organic frameworks (MOFs) led to the development of materials with controllable morphologies and tunable properties, such as moisture sorption, catalytic activity, thermal stability, and luminescence.

The proposed topic aligns with current international research interests in the field of hybrid and functional materials chemistry, particularly organosilicon compounds with biological activity, catalytic properties, selective metal ion complexation capabilities, and optical

properties. It addresses key research directions promoted by international platforms such as *Horizon Europe and initiatives focused on advanced materials*. At the national level**,** this research aligns with the strategic directions outlined in the National Research and Development Plan (PNCD), particularly in the fields of advanced chemistry and nanotechnologies. Moreover, the topic is consistent with the scientific interests and expertise of the research group within which the thesis was carried out, a team with established experience in silicon chemistry, coordination chemistry, and the development of hybrid materials for diverse applications.

The research hypothesis originated from the idea that the chemical bonding of siloxane and silane fragments with functionalized organic moieties—owing to their contrasting natures—would lead to hybrid compounds and materials exhibiting dual behaviors (*flexible–rigid, hydrophobic–hydrophilic, amorphous–crystalline*) and new properties that reflect this duality. Through the strategic selection of precursors, the functionality of the resulting compounds could be directed toward specific applications (*biology, environmental science, preparative chemistry, advanced materials*).

Scientific objectives:

- Synthesis of new bis-triazolic derivatives featuring siloxane and silane bridges *via thiol-alkylation reaction*s of *dihalogenated siloxanes and silanes with substituted mercaptotriazoles*; structural characterization, investigation of properties, metal ion coordination capacity, and biological activity.
- Functionalization with carboxyl or thioacetate groups of siloxane substrates (*disiloxanes, cyclotri- and tetrasiloxanes*) via *thiol-ene addition*; structural characterization and study of their surface, thermal, and electrical properties.
- Use of *carboxy-functionalized organosilicon compounds* for the complexation of metal ions; structural characterization, property evaluation, and identification of application potential of the resulting materials.

The research activities carried out to achieve these objectives, along with the results obtained, constitute the content of this thesis, the structure of which is presented below. The ***Introduction*** justifies the choice of the topic, highlighting its novelty and relevance, as well as its alignment with current national and international research interests.The research hypotheses and scientific objectives are formulated, and the particularities of the thesis are presented (methodology, results, degree of interdisciplinarity, limitations, and future perspectives). The

results of the activities carried out are organized into two parts: **PART I, "The current state of research in the thesis field**", consists of two chapters. **Chapter 1** contextualizes and defines the thesis domain, presents the types of organosilicon compounds and the aspects already explored, identifying relevant directions addressed internationally as well as within the laboratory where the thesis was developed, and research niches with potential in this field. **Chapter 2** presents the types of relevant reactions applicable for the chemical modification of organosilicons and the properties that can be conferred through these modifications.

The original contributions are the subject of **PART II**, which comprises six chapters, each with its own sections establishing the context and motivation of the study dedicated to a specific type of compound, as well as its own conclusions.**Chapter 3. Silanes/Disiloxanes Modified with Triazole Units** presents various structures of crystalline compounds obtained through thioalkylation reactions, exhibiting antibacterial and antifungal activity, as well as the ability to selectively bind Cu(II) ions, suggesting possible applications as chemical sensors and biologically active agents. **Chapter 4. Siloxane Derivatives Functionalized with Carboxyl/Tioacetate Groups** provides information on the synthesis of small-molecule silicon compounds functionalized with carboxyl/tioacetate groups via thiol-ene addition. These compounds are liquids with amphiphilic properties, self-assembly capability, low glass transition temperatures, and high dielectric constants, recommending them as potential solvent-free ionic liquid electrolytes for batteries. **Chapter 5. Copper Complexation with Policarboxylic Cyclosiloxanes** is devoted to the rapid and spontaneous complexation of copper ions in alcoholic solution, generating structures with stable spherical morphology, hydrophobic properties, and thermal stability. While policarboxylic cyclosiloxanes can be used as metal-extracting agents, the formed complexes can serve as efficient catalysts in organic reactions or agents with biological activity. **Chapter 6. Complexation of Aluminum with Siloxane-Dicarboxylic Acid** describes the synthesis of a MOF-type structure, an insoluble amorphous compound somewhat similar to the commercial aluminum fumarate *Basolite A520*, exhibiting hydrophobic character and low glass transition temperature. This compound is promising as a reinforcing material for silicones, resulting in a new silicon-based composite that was evaluated for morphology, mechanical, and optical properties.**Chapter 7. Manganese Complexation with Dicarboxylic Silane Acid** refers to a one-dimensional coordination polymer obtained by the self-assembly of *bis(p-carboxyphenyl)diphenylsilane* with Mn(II) ions under solvothermal conditions. The compound is

thermally stable and hydrophobic, with promising photophysical properties (violet-blue emission and transparency in the visible region). **Chapter 8. Experimental Section** presents the materials, working protocols, and characterization and testing techniques. **Chapter 9. General Conclusions** synthesizes the main results and original contributions of the research, highlights encountered challenges and proposed solutions, and finally estimates future directions for research development in the thesis field. The thesis concludes with a *list of publications and activities* related to the thesis domain and *References*.

In **Annexes I–IV**, data, figures, and supporting information for the reports in Chapters 3–6 of the thesis are presented.

PART II: ORIGINAL CONTRIBUTIONS

CHAPTER 3. SILANES/DISILOXANES MODIFIED WITH TRIAZOLE UNITS

3.2. Synthesis of Silicon Compounds Modified with Triazole Units

In this chapter, the S-alkylation of three mercaptotriazoles (*3-mercapto-1,2,4-triazole, 3-mercapto-4-methyl-1,2,4-triazole, and 3-mercapto-4-phenyl-5-methyl-1,2,4-triazole*) was carried out using two silicon-containing alkylating agents, *1,3-bis(chloromethyl)-1,1,3,3-tetramethyldisiloxane* and *bis(chloromethyl)dimethylsilane* (Scheme 3.1).

The association of siloxanes with triazoles via a thioether linkage represents a novel strategy for creating conjugated bis-triazoles.

While all other reagents are commercially available, 3-mercapto-4-phenyl-5-methyl-1,2,4-triazole (1 from Scheme 3.1) was synthesized and characterized in the laboratory (S3.1, Figures S3.1 - S3.3). The thioalkylation reactions (S3.2–S3.7) were carried out in the presence of K_2CO_3 *in acetone at reflux temperature*. The yields ranged from good to excellent, and the purity of the isolated products was high, as demonstrated by elemental analysis results (S3.2–S3.7).

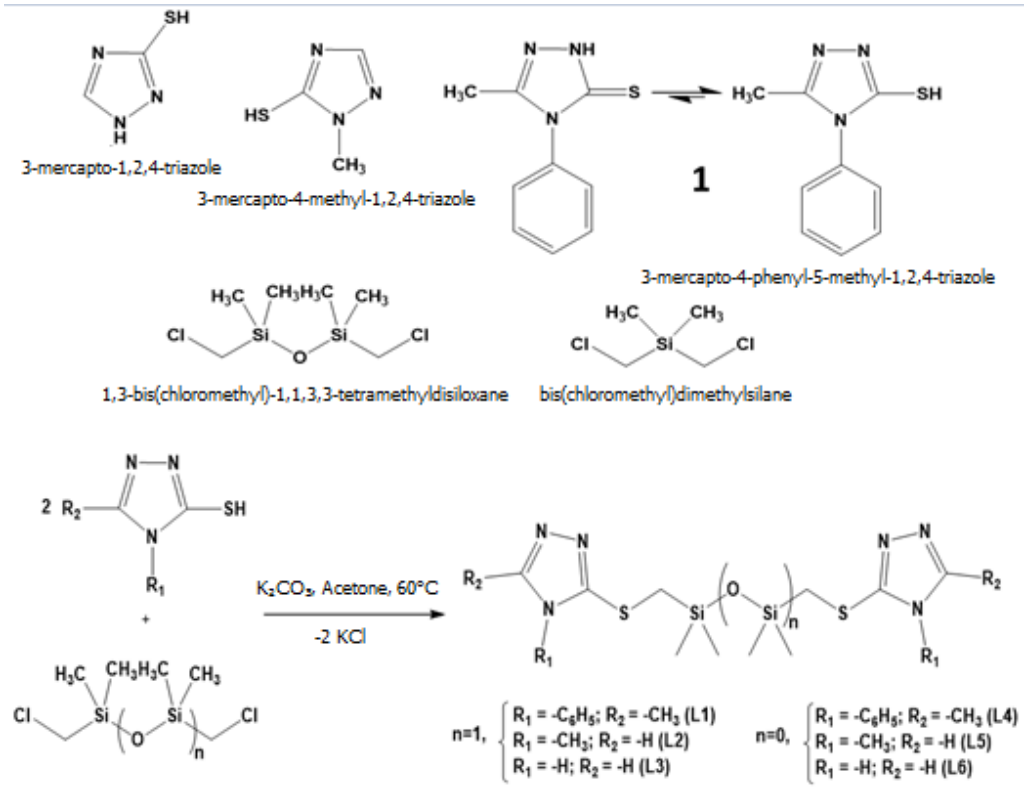

Scheme 3.1. Alkylation reaction of 3-mercapto-1,2,4-triazole derivatives with *1,3-bis(chloromethyl)-1,1,3,3-tetramethyldisiloxane* and *bis(chloromethyl)dimethylsilane* leading to compounds **L1 – L6**.

3.3. Structural characterization of silicon compounds modified with triazole units

3.3.3. Crystallographic analysis

The new silicon compounds containing triazole units **L1, L3–L6**, as well as the precursor **1** (*3-mercapto-4-phenyl-5-methyl-1,2,4-triazole*), being isolated in suitably crystalline form, were studied by single-crystal X-ray diffraction. Due to the high flexibility of the spacer, compounds with siloxane bridges can adopt either *trans* or *cis* conformations, while the silane derivatives exhibit a tetrahedral geometry.

The asymmetric units of the crystal structures of compounds **L4**, **L5**, and **L6**, containing the dimethylsilane spacer, are illustrated in **Figure 3.7**. In the crystals of compounds **L4** and **L5**, the packing of neutral molecules shows the presence of a two-dimensional supramolecular network, as seen in **Figure 3.8**. In the case of compound **L4**, 2D layers are formed due to intermolecular π–π interactions between centrosymmetric triazole rings at a distance of 3.447 Å (**Figure 3.8a**). For the crystal of compound L5, the formation of the 2D wave-like network is directed by intermolecular C–H•••N hydrogen bonds (**Figure 3.8b**).

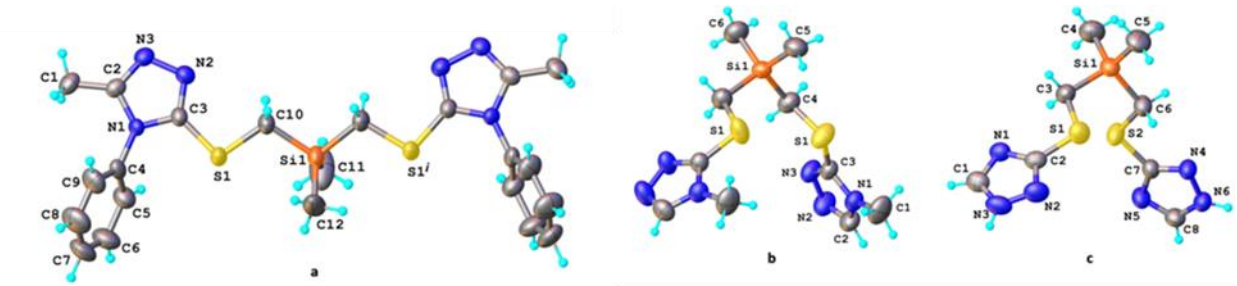

Figure 3.7. X-ray molecular structure of: a) compound **L4**; b) compound **L5**; c) compound **L6**, with labeled atoms and thermal ellipsoids at 50% probability.
Symmetry code i): 1 – x, y, z.

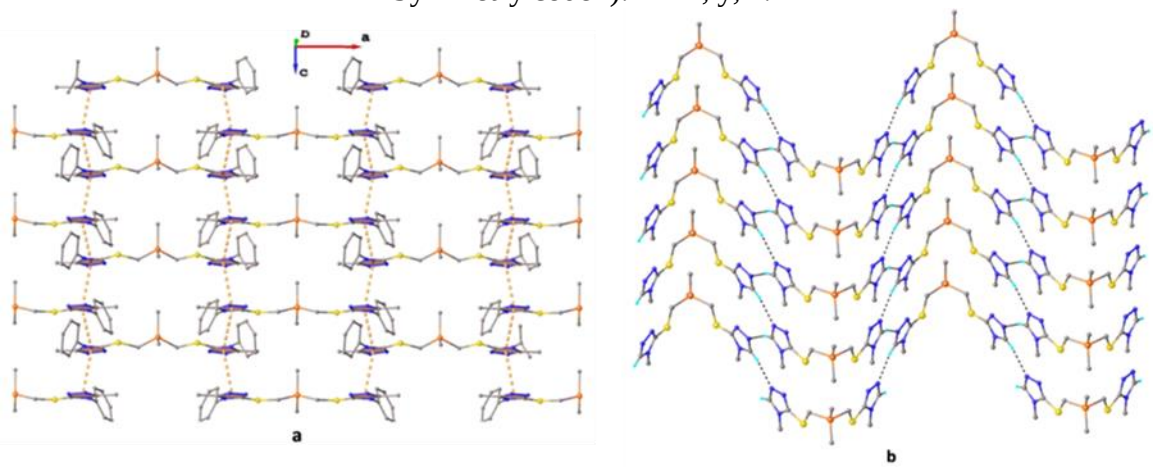

Figure 3.8. Image of the two-dimensional supramolecular architecture in the crystal structure of **L4** (a) and **L5** (b). Centroid-to-centroid distances and hydrogen bonds are represented by orange and black dashed lines. Irrelevant hydrogen atoms are omitted. Hydrogen bond parameters: C2-H•••N2 [C2-H 0.93 Å, H•••N2 2.501 Å, C2-H•••N2 (1,5 – x, y – 0.5, 1 – x) 3.406(3) Å, ∠C2HN2 164.4°].

3.4. Study of the properties of silicon compounds modified with triazole units

3.4.2. Evaluation of the metal ion binding capacity

Initially, the cation binding capacity was studied by monitoring changes in absorption spectra during the titration of triazole derivatives with a $CuCl_2$ solution in methanol. The absorption spectra of the triazolic derivatives **L1–L6**, recorded in methanol solution (Figure 3.10), reveal a maximum at 240–257 nm, attributed to π-π* transitions within the triazole ring. The addition of varying volumes of 0.1 mM $CuCl_2$ solutions (ranging from 0.05 to 2 mL) caused a red shift of 12–20 nm in the band associated with the triazole ring. This new band was attributed to LMCT (ligand-to-metal charge transfer; dπ(Cu(II)) → π*(L)), confirming the

coordination of the Cu^{2+} ion by the triazole ring.

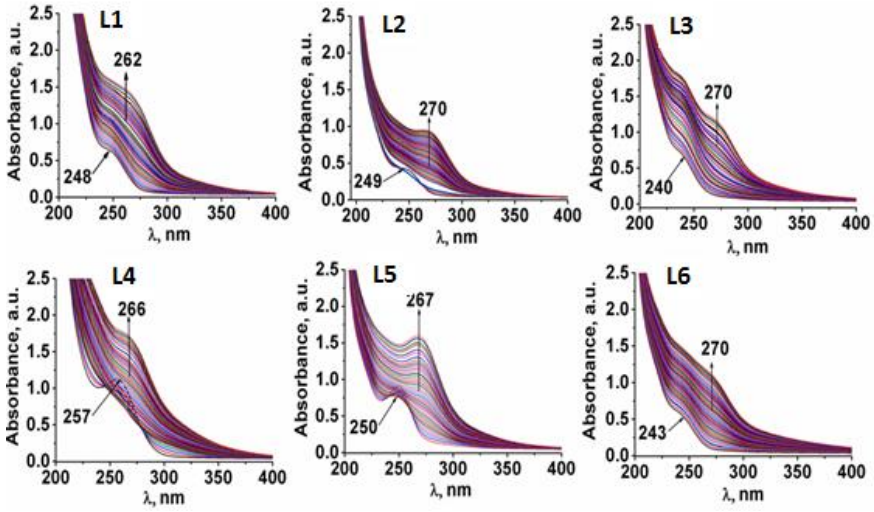

Figure 3.10. Changes in the UV-Vis spectra of triazole derivatives **L1–L6** during titration with $CuCl_2$ solution ([Cu^{2+}] mol/L between 1.75×10^{-6} and 1.04×10^{-4}).

The sensing properties of the bis-triazoles **L1–L6** were also tested under the same conditions against Mn^{2+} and Zn^{2+}, the first and last elements in Irving's series (Irving, 1953), but no shift in the absorption maximum or the appearance of a new band was observed after the sequential addition of increasing volumes of solutions containing Zn^{2+} or Mn^{2+} to the bis-triazole solution. Therefore, the bis-triazoles **L1–L6** demonstrate a high selectivity toward Cu^{2+} in methanolic solution.

3.4.3. Evaluation of Antimicrobial Activity

Given that triazole derivatives form the basis of many anti-infective and antifungal drugs—such as *fluconazole, voriconazole, itraconazole, and posaconazole* (Ayati, 2016)—*in vitro* tests were conducted for compounds **L1–L6** to evaluate their antibacterial and antifungal activity. These tests targeted five types of fungal cultures (*Aspergillus niger*, *Penicillium frequentans*, *Penicillium fumigatus*, *Alternaria alternata*, *Fusarium*) as well as Gram-negative bacteria (*Pseudomonas aeruginosa*) and Gram-positive bacteria (*Bacillus polymyxa*). The minimum inhibitory concentration (MIC) values obtained are presented numerically in Table S3.1 (Appendix 1) and graphically in Figure 3.14.

Among the tested compounds, the best biological activity was recorded for compound **L6** at a concentration of 1.5% in chloroform, under which conditions it was more active than the reference drugs. The *MIC* values for this compound are 0.006 μg/mL for all types of fungi,

compared to 0.3 µg/mL for caspofungin. At the same time, the *MIC* values are 0.064 µg/mL for both bacterial species, compared to 3.5 µg/mL for kanamycin. In contrast, the antimicrobial activity of compound **L6** in methanolic solutions is significantly lower, with *MIC* values of 0.75 µg/mL for fungi and 64 µg/mL for bacteria. Compounds **L2** and **L4** showed good antibacterial activity (*MIC* values of 0.094 and 0.25 µg/mL, respectively) and antifungal activity (*MIC* values of 0.098 and 0.012 µg/mL, respectively) when tested in 1.5% chloroform solution. Compound **L1** exhibits antimicrobial activity that is similar or comparable to that of the reference drugs.

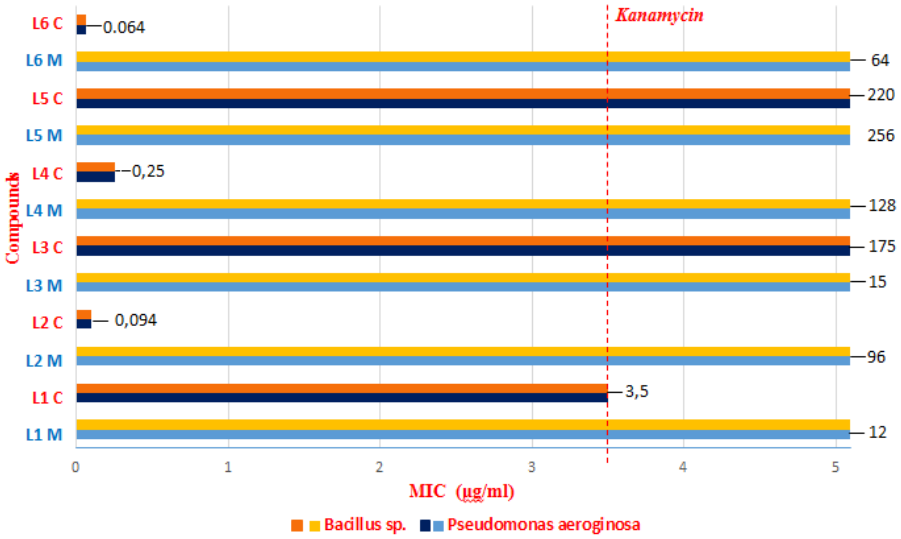

(a)

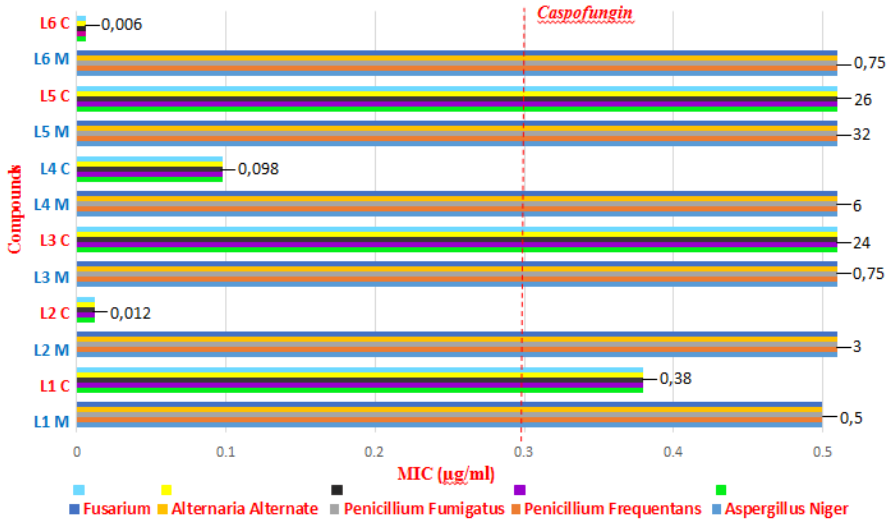

(b)

Figure 3.14. Comparative representation of the antibacterial (a) and antifungal (b) activities (expressed as MIC values) of bis-triazoles **L1–L6** as 1.5% solutions in methanol (M) and chloroform (C).

3.4.4. Evaluation of the Hydrophilic-Lipophilic Balance (HLB)

Given that previous studies conducted on various types of 3-mercapto-1,2,4-triazole derivatives have shown that antibacterial activity is correlated with dipole moment values (Plech, 2013), the dipole moments of the newly synthesized compounds **L1–L6** were calculated using the HF/LanL2DZ method. The obtained values are graphically represented in Figure 3.15.

As can be observed, in the series of compounds with a siloxane spacer (compounds **L1–L3**), the dipole moment increases from the *3-mercapto-4-phenyl-5-methyl-1,2,4-triazole derivative* to *3-mercapto-4-methyl-1,2,4-triazole* and *3-mercapto-1,2,4-triazole*. In contrast, in the series with a silane spacer, the trend is disrupted by compound **L5**, derived from *3-mercapto-4-methyl-1,2,4-triazole*. As a result, these values alone cannot explain the high antibacterial activity of compound L6, for example. Conformational factors could also be responsible for this hierarchy. Therefore, the hydrophilic-lipophilic balance (*HLB*) was calculated using the Griffin (Griffin, 1949; Griffin, 1954) and Davies (Davies, 1957) formulas: ***HLB = (mass % of hydrophilic groups) / 5.***

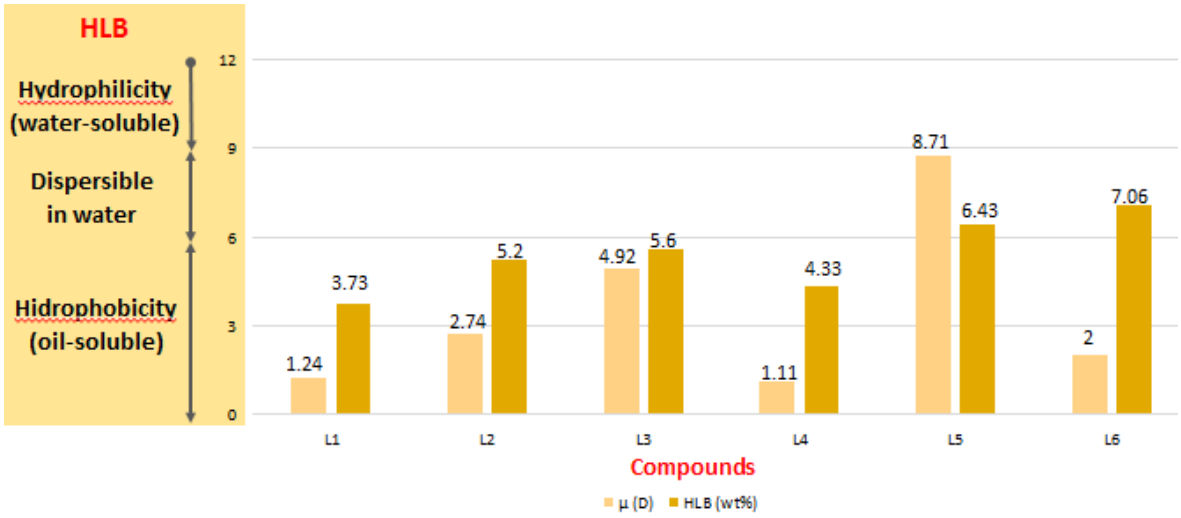

Figure 3.15. Comparative graphical representation of the dipole moment values (μ) calculated using HF/Lan2DZ theory and the hydrophilic-lipophilic balance (HLB) of compounds **L1–L6.**

The values obtained, shown graphically in Figure 3.16, range between 3.73 and 7.06, characteristic of hydrophobic compounds that include materials from water-insoluble to water-dispersible. Compound **L6** has the highest HLB value (7.06), being the strongest candidate for surfactant properties among the series of compounds, consistent with the behavior reported in ref. (Davies, 1957). For the other active compounds, **L2, L4**, and **L1**, antibacterial activity

decreases with decreasing *HLB* values. None of the analyzed compounds show significant antimicrobial activity in methanol, while in chloroform they are very active. This suggests that the solvent, which can influence conformation and self-assembly factors, is responsible for the observed biological activity.

CHAPTER 4. SILOXANE DERIVATIVES FUNCTIONALIZED WITH CARBOXYL/THIOACETATE GROUPS

4.2. Functionalization of siloxane derivatives with carboxyl/thioacetate groups

For the first time in this case, substrates used included a disiloxane with one vinyl group on each silicon atom, **V2** – *1,3-divinyl tetramethyldisiloxane*, a cyclosiloxane with three siloxane units, **V3** – *1,3,5-trivinyl-1,3,5-trimethylcyclotrisiloxane*, and one with four siloxane units, **V4** – *2,4,6,8-tetramethyl-2,4,6,8-tetravinylcyclotetrasiloxane*, which were subjected to the thiol-ene addition reaction. As sources of carboxylic groups, the following were used: **R1** – *3-mercaptopropionic acid*, **R2** – *thioglycolic acid*, and **R3** – *thioacetic acid* (Scheme 4.1).

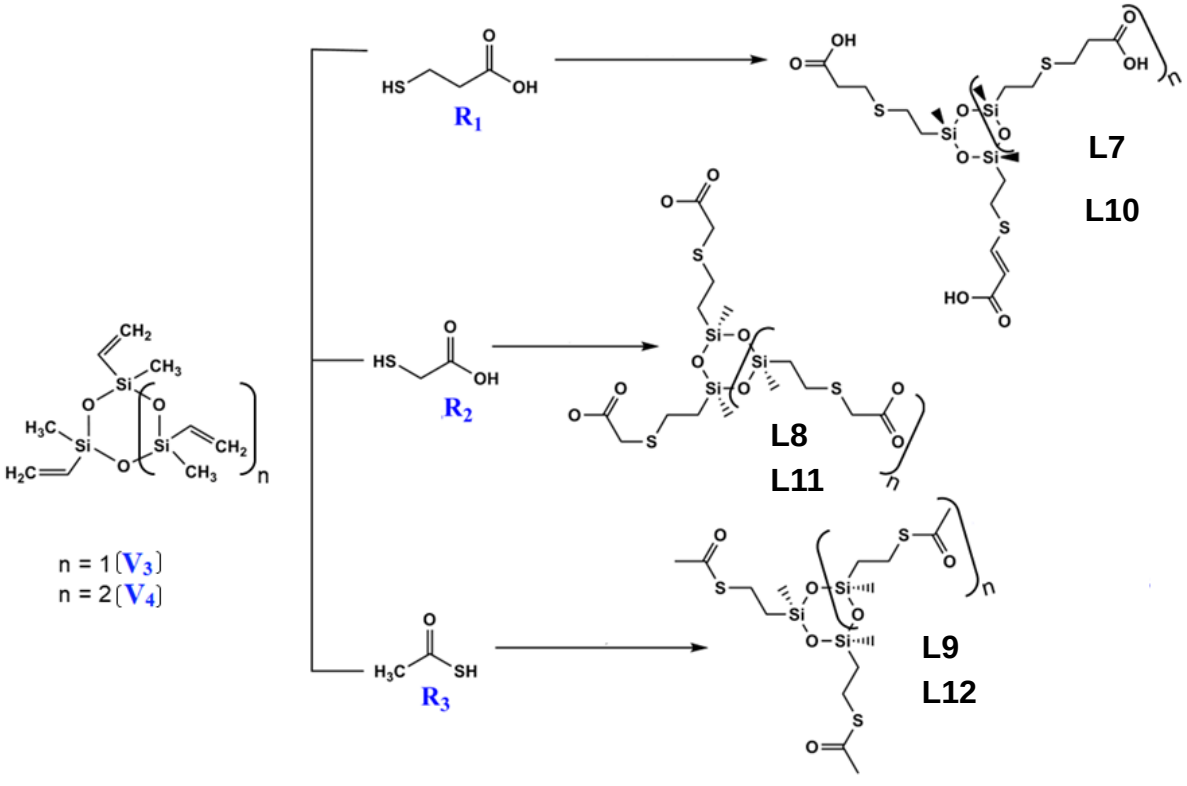

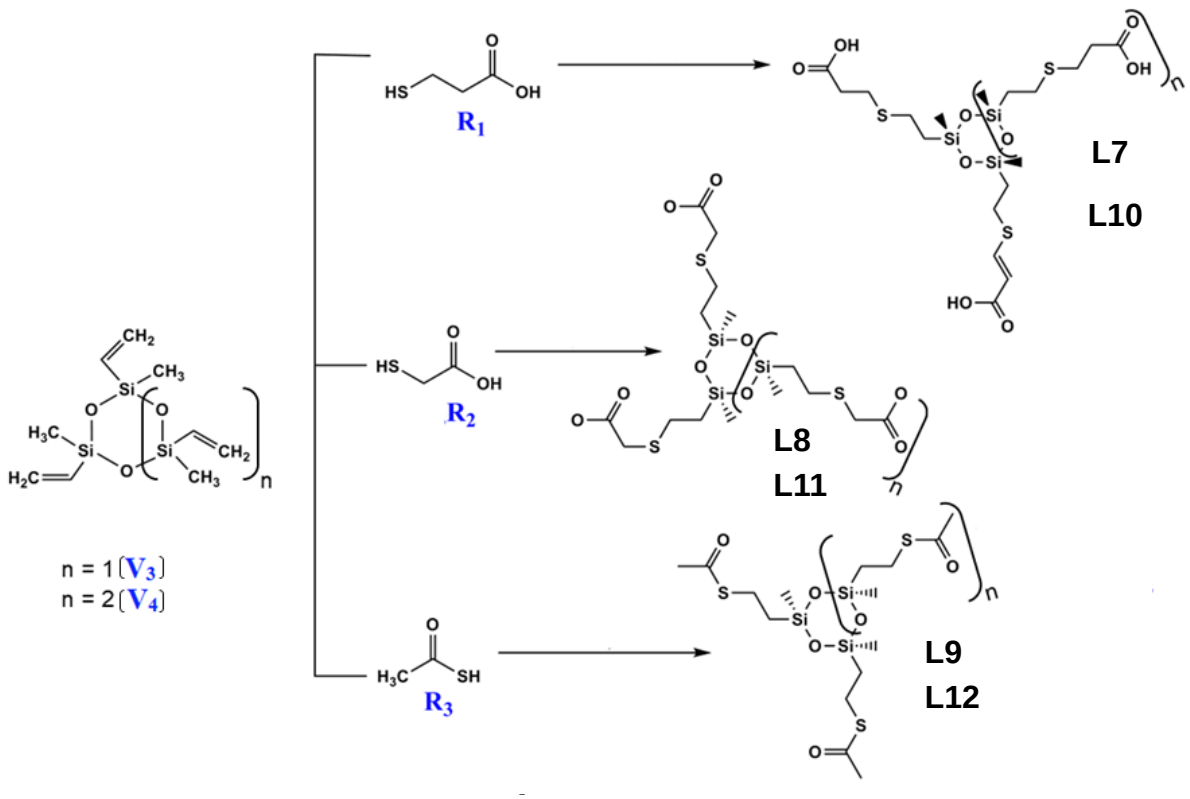

Scheme 4.1. Functionalization of silicon derivatives with carboxyl groups via thiol-ene addition.

The working protocol illustrated consists, in principle, of mixing the silicon substrates (**V2**, **V3**, or **V4**) with the thiol derivatives (**R1, R2**, or **R3**) in a molar ratio of 1:1.1 (vinyl:thiol groups) in *tetrahydrofuran (THF).*To activate the reaction thermally or photochemically, *2,2'-azobis(isobutyronitrile) (AIBN)* and *2,2-dimethoxy-2-phenylacetophenone (DMPA)* were added to the reaction mixture as thermal and photochemical initiators, respectively. For the thermally activated reaction, the mixture was refluxed at the boiling point of the solvent for 3 hours under magnetic stirring, after which the volatile fractions (mainly solvent and excess thiol derivative) were removed by vacuum distillation. In the case of the photochemically activated reaction, the reaction mixture was exposed to UV irradiation at $\lambda = 320$ nm**.**

4.3. Structural characterization of functionalized siloxane derivatives

4.3.1. Fourier transform infrared spectroscopy (FTIR)

The progress of the thiol-ene addition reaction was initially monitored by IR spectroscopy (Figure 4.2a, Annexe 2), tracking the disappearance of the absorption bands corresponding to the

C-H bond in the vinyl groups, at 3057 and 1597 cm^{-1} in **V3**, 3055 and 1597 cm^{-1} in **V4**, and 3057 and 1597 cm^{-1} in **V2**, as well as the bands at 2666 and 2567 cm^{-1} corresponding to the S-H bond in the mercapto-derivatives (Cao, 2014). In the spectra of the reaction products, the medium band at 1416–1420 cm^{-1} and the weak band at 2850 cm^{-1} can be associated with the (S-)CH_2- bonds (asymmetric stretching and δ bending, respectively) (Pretsch, 2009). Additionally, the band corresponding to the carboxyl group ν_as (C=O) is present around the same value (1711 cm^{-1}). as in the starting thiols (1709 cm^{-1}), as well as the characteristic bands of the dimethylsiloxane unit: ν_s(Si-O-Si) in the range 1010–1090 cm^{-1} and 1256 cm^{-1} assigned to ν(Si-CH_3). It is well known that a specific absorption band corresponding to ν(Si-O-Si) appears at 1010–1020 cm^{-1} in cyclic siloxane trimers, at 1070–1090 cm^{-1} in tetramers, while for higher members of the series this band broadens and splits (Launer, 1987; Racles, 2017). The shape and position of the ν(Si-O-Si) absorption band at 1074, 1078, and 1078 cm^{-1} in the spectra of compounds **L10–L12,** at 1015, 1013, and 1013 cm^{-1} in the spectra of products **L7–L9**, and at 1053, 1059, and 1062 cm^{-1} in the spectra of compounds **L13–L15** indicate tetrameric, trimeric, and dimeric species, respectively (Figure 4.2b). The formation of the structures is also supported by the NMR analysis data.

4.4. Evaluation of material properties of policarboxylated siloxane compounds

4.4.1. Study of surface properties and self-assembly capacity

Starting from the hypothesis that the presence of both a nonpolar part and polar groups within the same molecule leads to a tendency for association and self-assembly, this phenomenon was also investigated for the compounds reported in this chapter. The presence of aggregates is demonstrated by *nanoparticle tracking analysis (NTA)* performed in solution using the NANOSIGHT equipment. With the help of this technique, a series of video images were recorded, and Figure 4.4 illustrates the aggregation in solution for compound **L8**, along with the particle size distribution. The analysis was carried out using concentrated (10%) solutions of the polysiloxane polycarboxylate compound, and the average particle size estimated by this technique is slightly larger than that estimated by *DLS* (for example, 293 nm compared to 200nm).

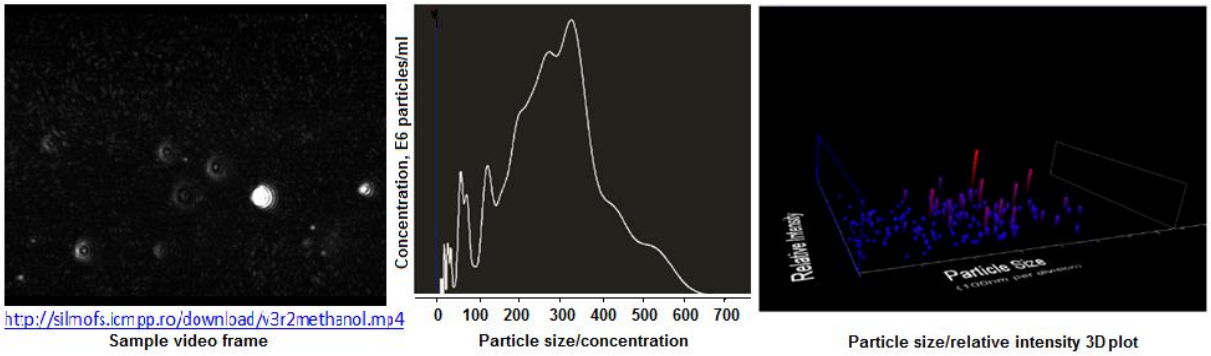

Figure 4.4. Aggregation in solution highlighted by nanoparticle tracking analysis (NTA) for **L8** 10% in methanol (average particle size: 293 nm)

The dynamic sorption-desorption isotherms of water vapor (Figure 4.5) indicate, for example, that the L10 sample exhibits a mass gain of 6.82% at maximum humidity (RH – 90%), and the amount of retained water is completely released during desorption, with the sample returning to its initial mass. This moisture sorption value can be considered modest, given the high density of extremely polar carboxyl groups in the compound. This hydrophobicity can be attributed to the methyl groups, which always migrate to the air interface, thus forming a barrier to water vapor.

4.4.3. Dielectric Response

The presence of carboxyl groups in high proportion in the compounds, either in liquid or molten state under normal conditions, creates the premise for their functioning as solvent-free liquid electrolytes. Interest in polysiloxane-based electrolytes dates back to the 1980s, particularly focusing on polysiloxanes substituted with *polyethylene oxide (PEO*). Their ionic conductivity is attributed to the flexible segment that ensures the polymer remains completely amorphous (Zhang, 2005). Figure 4.7 presents a comparative variation of the dielectric constant ε', which is associated with the energy stored in a material due to the dielectric polarization of dipoles, as a function of frequency for pure vinylsiloxane derivatives and their products obtained by thiol-ene addition, either as such (represented by open symbols) or doped with Li (represented by filled symbols). The vinylsiloxanes **V3, V4**, and **V2** (due to their nonpolar character), taken as references, show the lowest dielectric constant values across the entire frequency range because of their nonpolar nature. As expected, the dielectric spectrum shows an increase in both dielectric permittivity and conductivity from vinylsiloxanes to the thiol-ene addition products and, more significantly, to the lithium-doped derivatives. The values of the electrical parameters combined

with their physical state (viscous liquids) and thermal stability under normal conditions create the premise for their suitability for use as solvent-free liquid electrolytes in ionic batteries.

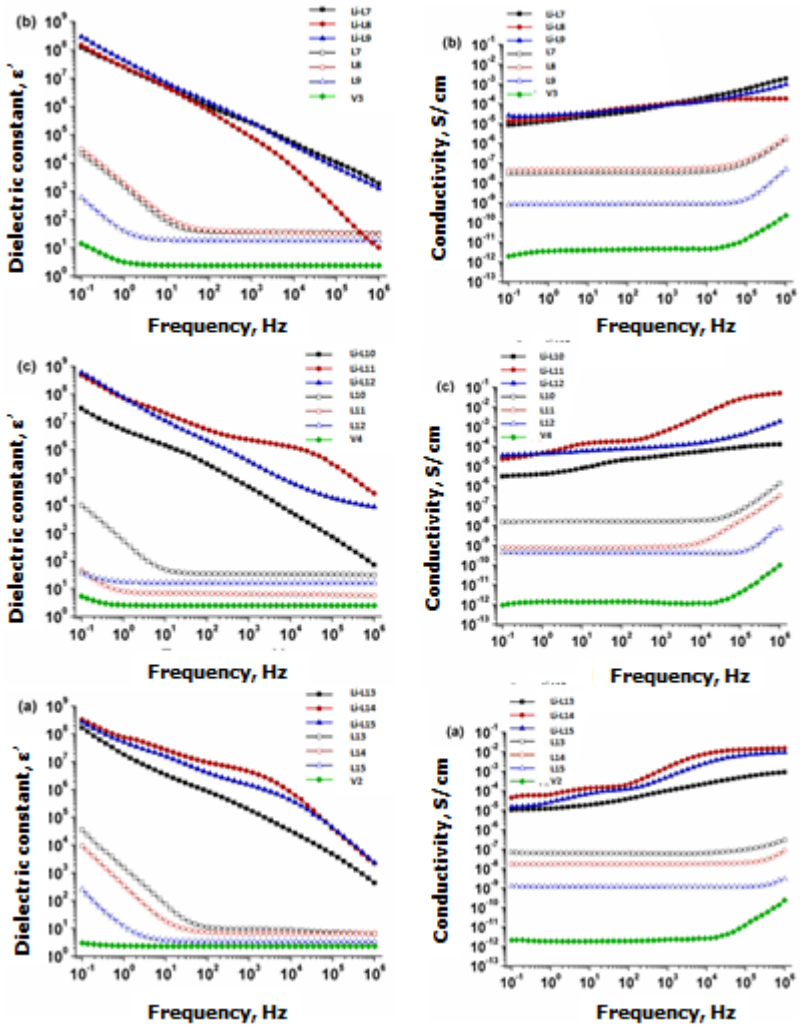

Figure 4.7. Representation of dielectric permittivity (left) and conductivity (right) as a function of frequency for the pure siloxanes: a-**V2**, b-**V3**, c-**V4**, their obtained derivatives, and lithium-doped products.

The values of the electrical parameters, combined with their physical state (viscous liquids) and thermal stability under normal conditions, provide a basis for their suitability as solvent-free liquid electrolytes in ionic batteries. According to literature studies (Georén, 2003), an amphiphilic electrolyte could improve electrochemical properties—such as electrochemical stability and charge transfer resistance—of a battery electrode, due to its specific surface properties.

CHAPTER 5. COPPER COMPLEXATION WITH POLYCARBOXYLIC CYCLOSILOXANES

5.2. Complexation of copper ions with polycarboxylic cyclosiloxanes

In this thesis, the synthesis and properties of new copper complexes of cyclosiloxanes functionalized with carboxyl groups, presented in Chapter 3.2, are reported.

For this study, three heterocyclic (siloxane) compounds were selected, which differ from each other both in ring size and in the length of the spacer between the carboxyl group and the silicon atom to which it is attached.The structures of the three compounds considered, **L7, L8**, and **L10**, are shown in Scheme 5.1. Alcoholic solutions (methanol or ethanol) with a concentration of 10% of the three ligands **L7, L8**, and **L10** were prepared. These solutions were treated with a slight excess of copper acetate (molar ratios VnRm:$Cu(Ac)_2$ = 1:3.3, 1:3.3, and 1:4.4, respectively) dissolved in methanol to form 10% solutions. The copper acetate solution was slowly added dropwise along the walls of the vessel at room temperature. Instantly, a blue-green precipitate formed and deposited in the case of compounds **L7Cu** and **L10Cu**, and an emerald green precipitate formed in the case of compound **L8Cu**, while the liquid phase remained blue due to the excess copper acetate.

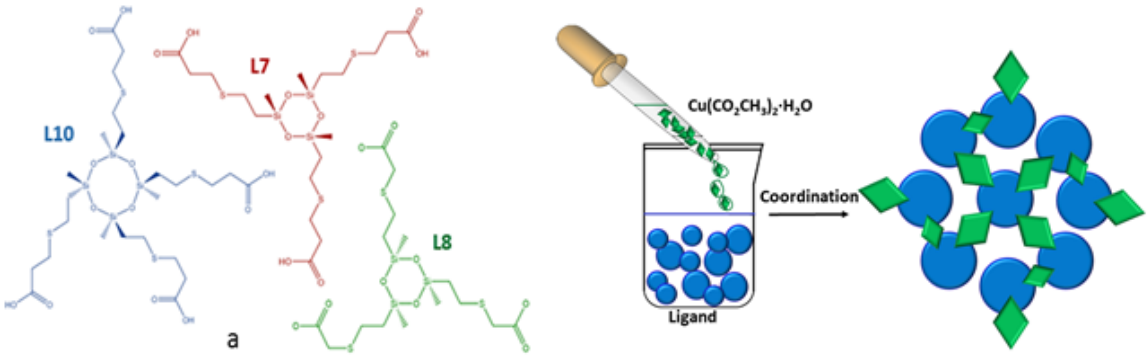

Scheme 5.1. Siloxane derivatives functionalized with multiple carboxylic groups used as ligands (a); schematic representation of the preparation method of metal complexes of the ligands with a ciclosiloxane backbone (b).

5.3. Structural characterization of copper complexes

The coordination mode and structure of the complexes were studied by *FTIR* and *diffuse reflectance UV-Vis* (*DRS*) *spectroscopy*, *energy-dispersive X-ray spectroscopy* (*EDX)*, and *wide-*

angle X-ray diffraction (WAXRD), while the morphology was analyzed by *electron microscopy (TEM, SEM)*.

5.3.2. Energy-Dispersive X-ray Spectroscopy (EDX)

The results of the EDX analyses for the obtained coordination compounds (Figure 5.5) indicate for Si and Cu—key elements in elucidating the coordination ratio—a molar ratio of approximately 2:1 in all three cases, as expected for a 100% complexation degree.

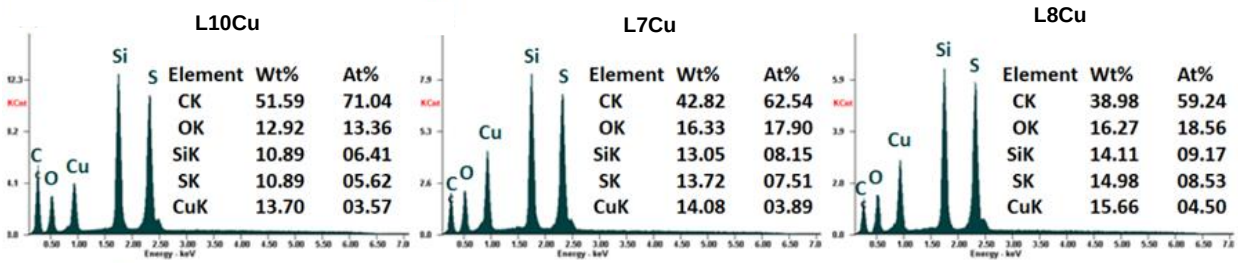

Figure 5.5. EDX spectra for copper complexes.

Therefore, regardless of the coordination mode, the copper ion is coordinated by four oxygen atoms belonging to two or more carboxyl groups which, depending on conformation and steric factors, may originate from the same molecule or from neighboring ligand molecules. Additionally, acetate groups are present in the complex attached to the metal, either in a bidentate or chelating mode.

5.3.5. Morphological study of copper complexes

The isolated products were analyzed morphologically by *SEM* and *TEM* (Figures 5.8, 5.9).

The *SEM* images reveal, in all three cases, a free-sphere type morphology, with more or less polydisperse sizes (Figure 5.8). The detail in Figure 5.8d (green inset) indicates solid spheres. The *TEM* images also reveal a morphology consisting of size-polydisperse spheres, which are rarely interconnected, as can be observed in Figure 5.9, where illustrative images for compounds **L10Cu** and **L8Cu** are presented. During the measurements, it was noted that the samples were resistant to the electron beam, indicating a high inorganic content. The *STEM* analysis (Figure 5.9b), which provides greater contrast by highlighting differences in electron densities, suggests that the spheres are solid, while the diffraction pattern indicates crystallinity.

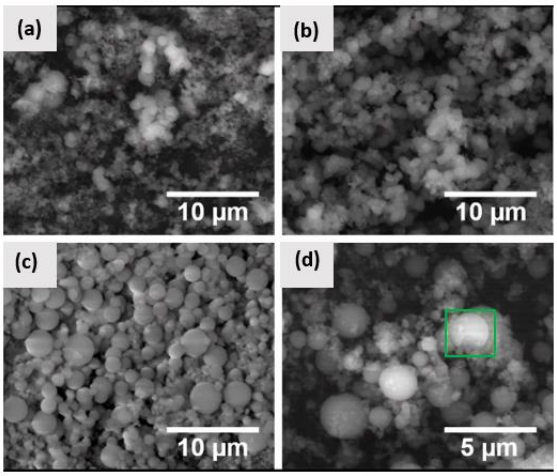

Figure 5.8. SEM images of Cu(II) complexes: a) L10Cu, b) L7Cu, c,d) L8Cu

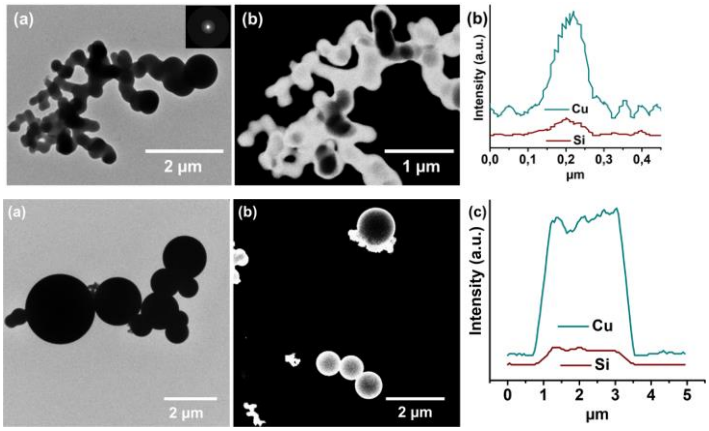

Figure 5.9. TEM (a) and STEM (b) images exemplified for the samples: L10Cu (top) and L8Cu (bottom); EDS lines indicate the presence of silicon and copper (the high copper content is due to the TEM grid).

The presence of aggregates is also demonstrated by in situ video recordings obtained using the *nanoparticle tracking analysis (NTA)* technique in ligand solutions, illustrated for compound **L8** in Figure 5.11, along with the particle size distribution. As can be seen, a relatively broad size polydispersity was detected.

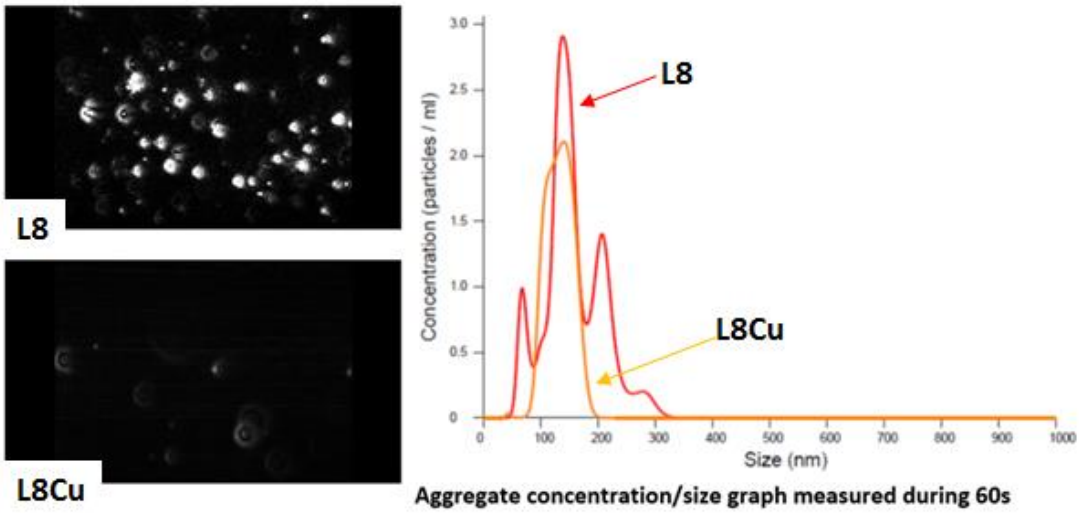

Figure 5.11. Visualization of aggregation in solution (10% concentration in methanol) using the NANOSIGHT equipment, exemplified for ligand **L8** and the copper complex **L8Cu** during its formation by simply mixing the ligand with copper acetate (video access: http://www.icmpp.ro/nta/nta1.mp4 and http://www.icmpp.ro/nta/nta2.mp4).

5.4. Study of the properties of copper complexes

Moisture and thermal behavior, as well as antifungal and catalytic activity, were studied.

5.4.2. Thermal behavior

Thermogravimetric analysis (Figure 5.15) indicates very similar decomposition patterns for the L10Cu and L7Cu samples, which share the same carboxylic ligand (*3-mercaptopropionic acid*), exhibit very similar patterns, while the *L8Cu* complex, based on a ligand with shorter arms (*thioglycolic acid*), behaves slightly differently. This suggests that thermal stability is influenced by the nature/length of the spacer between the silicon atom and the carboxyl group of the ligand. The samples decompose in four stages, with the main decomposition step peaking at 193 °C for the **L10Cu** and **L7Cu** complexes and at 183 °C for the **L8Cu** complex. Additionally, **L8Cu** shows a mass loss around 60 °C, which is attributed to the release of retained solvent. The DSC curves do not indicate the presence of any transitions above room temperature (Figure 5.15b).

5.4.4. Catalytic Activity

Since the metal cation is typically located at the hydrophilic–hydrophobic interface of the aggregate, metal surfactants are of interest in organic catalysis, where they can interact with both hydrophilic and hydrophobic substrates. The three synthesized copper complexes were used to activate the decomposition reaction of H_2O_2, which is known to be of significant practical interest (Brown, 1993; Skounas, 2010; Racles, 2016). The testing method used was the gasometric method (Goldstein, 1974). A graphical representation of the H_2O_2 conversion (%) as a function of time (s), in the presence of the three copper complexes **L7Cu, L8Cu**, and **L10Cu** as catalysts in alkaline medium, is shown in Figure 5.18a. The curves were recorded up to a conversion of 25%, which was the maximum allowed by the setup. This conversion value (25%) was reached the fastest in the presence of compound **L7Cu** (90 s), followed by compound **L8Cu** (165 s), and much more slowly in the presence of compound **L10Cu** (4140 s). Since catalytic activity depends on several factors, such as the accessibility of H_2O_2 to the catalytic species, in the case of copper complexes a correlation was observed between catalytic activity and the number of available coordination sites (Brown, 1993).

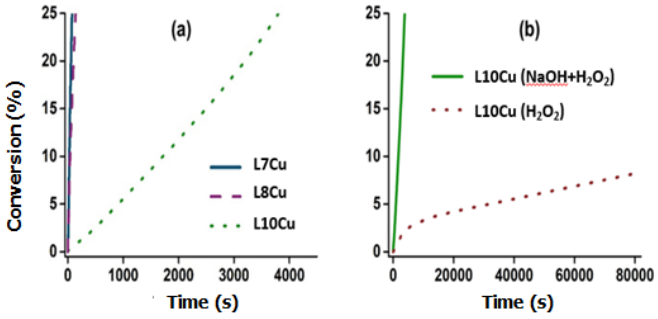

Figure 5.18. Comparative representation of the H_2O_2 decomposition reaction conversion catalyzed by the three copper complexes under standard temperature and pressure conditions: (a) in alkaline medium; (b) in water at neutral pH.

In this case, as can be observed, the copper complexes based on cyclotrisiloxane ligands, **L7Cu** and **L8Cu**, are much more active than the compound based on the cyclotetrasiloxane ligand **L10Cu**. This could be attributed to the existence of free coordination sites in the former, which remain due to the conformational constraints imposed by the planarity of the trisiloxane ring. The catalytic activity was also tested without using NaOH (Figure 5.18b).

It is stated that in simple Cu(II)/H_2O_2 systems, in neutral medium, the concentrations of short-lived reactive species are too low to be accurately evaluated (H. Lee, 2016). As expected, the catalytic activity drastically decreased when the reaction medium was neutral. Analyzing our results, for example, after 60 minutes, the compound **L10Cu** decomposes 23.2% of the initial H_2O_2, while at neutral pH only 2.1%. After 22 hours of using **L10Cu** in a neutral pH medium, approximately 8% of H_2O_2 was decomposed. However, the volume of oxygen released is reasonable and could create an adequate oxidative environment for certain reactions. The compound **L8Cu** shows no activity in neutral medium.

CHAPTER 6. COMPLEXATION OF ALUMINUM WITH SILOXANE-DICARBOXYLIC ACID, AlSiA

6.2. Coordination of aluminum ions with siloxane-dicarboxylic acid, SiA

The literature-reported protocol for the synthesis of aluminum fumarate (e.g., *Basolite A520*) (Alvarez, 2015) was adapted by replacing fumaric acid with a silicon-containing dicarboxylic derivative (*1,3-bis(carboxypropyl)tetramethyldisiloxane, SiA*) as an alternative to the aliphatic acid, to obtain a new compound, ***AlSiA***. The procedure consists of adding an aqueous solution of SiA with excess NaOH, preheated to 60°C, by injection into the aluminum sulfate solution. A white precipitate forms instantly, which is isolated by vacuum filtration, washed with water to remove excess NaOH, then washed with acetone, and finally dried.

6.4. Preparation and isolation of the aluminum complex, AlSiA

The siloxane-dicarboxylic acid obtained previously was converted into its salt by mixing with an excess of NaOH (molar ratio SiA:NaOH of 1:3), and the resulting solution was added to an aqueous solution of *aluminum sulfate* in a molar ratio of 2:1, forming a white suspension. The solid phase was isolated, purified, and characterized by appropriate methods. Analyses (FTIR

and ^{1}H NMR in gel state in chloroform) indicated an isostructural character with the fumaric acid-based MOF, Basolite A520 (Stock, 2014), or with another aluminum coordination polymer (Krüger, 2017) (Scheme 6.1). In any case, the spacer length in ***AlSiA*** (11 atoms) and its high flexibility create the premises for interpenetration and/or collapse, as demonstrated in other cases (Bruce, 2011) where the spacer was extended to increase the distance between nodes and thus increase porosity, but the effect was the opposite. This is also indicated by porosity analysis data and water vapor sorption of this compound.

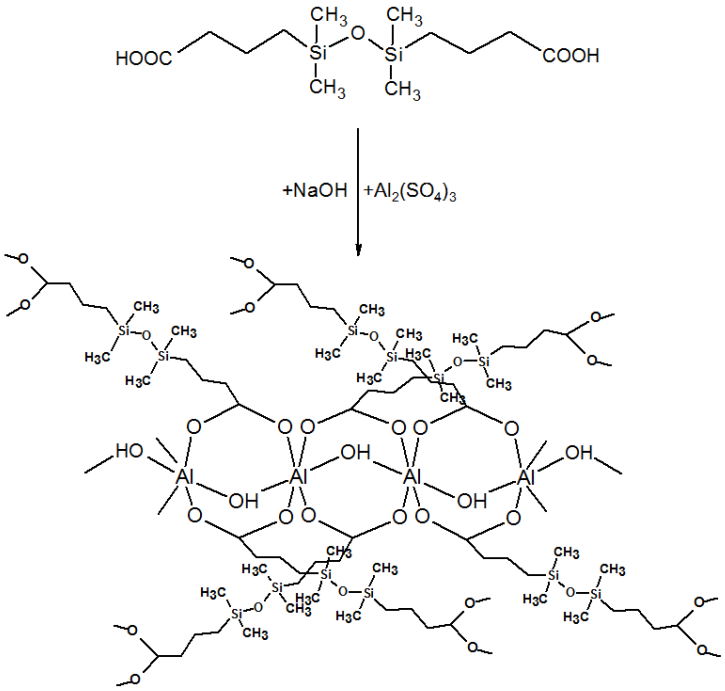

Scheme 6.1. Reaction scheme and probable structure of **AlSiA**.

6.5. Morphological and structural characterization of the aluminum complex

6.5.1. Study of the complex morphology

TEM images (Figure 6.4) of the sample deposited on a grid as a dispersion in ethanol show a series of roughly spherical particles, either isolated or aggregated, with sizes on the order of several hundred nanometers (Figure 6.4a).

This morphology, different from that of ***AlFA*** (Figure 6.5), may be dictated by the amphiphilic nature of the ligand. In water or any other polar medium, the ligand adopts a conformation that minimizes exposure of the hydrophobic segment, forming spherical aggregates with polar parts on the outside, where aluminum ions are coordinated. In the dry state, due to

very low surface tension, the highly flexible tetramethyldisiloxane segments migrate to the air interface, leaving the metal units (SBU) complexed inside the assembly, as much as structural constraints allow. The *TEM-EDX* line scan along the aggregates indicates the presence of both aluminum and silicon, the latter in high concentration, as also shown by elemental analysis results (Figure 6.4b). In the *PXRD diffractogram* (Figure 6.4c), besides the amorphous phase, peaks at 5° and 15° can be observed, indicating some degree of supramolecular organization.

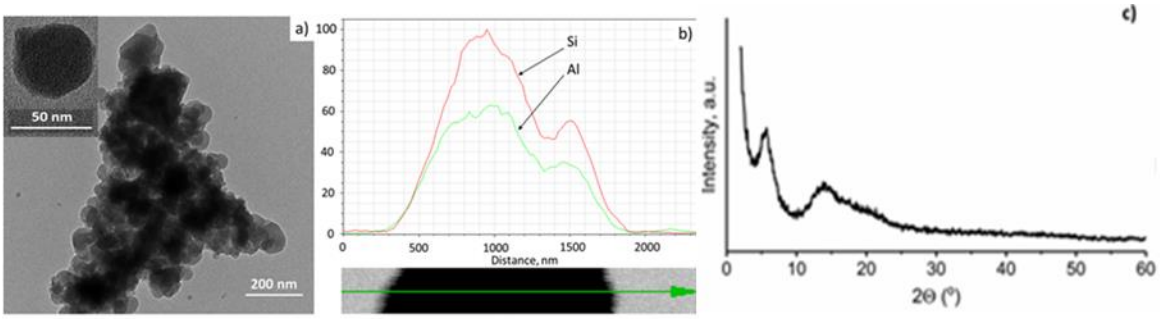

Figure 6.4. TEM image of the ***AlSiA*** sample dispersion (a); TEM-EDX line scan on the ***AlSiA*** formations (b); XRD pattern of the AlSiA sample (c).

6.7. Silicon composite with added aluminum complex AlSiA

Taking into account the low performance of the compound in terms of gas adsorption capacity at normal pressure, an alternative use for **AlSiA** was explored, namely as a *filler material for silicones.* Considering that the obtained product is built with a siloxane ligand, there are premises for good compatibility with a silicone matrix. Consequently, the compound was incorporated at 10 wt% into a solution of *polydimethylsiloxane* in toluene, and the mixture was ultrasonicated to ensure good homogenization. A crosslinking agent and a catalyst were then added to the reaction mixture, which was subsequently cast as a film. Through the reaction of the tetrafunctional crosslinking agent, *TEOS*, with the Si-OH chain ends of the siloxane chains, a network is formed that incorporates particles between the chains, resulting in elastomeric nanocomposites. After curing, the film was analyzed in terms of optical (Figure 6.11a-insert) and mechanical properties.

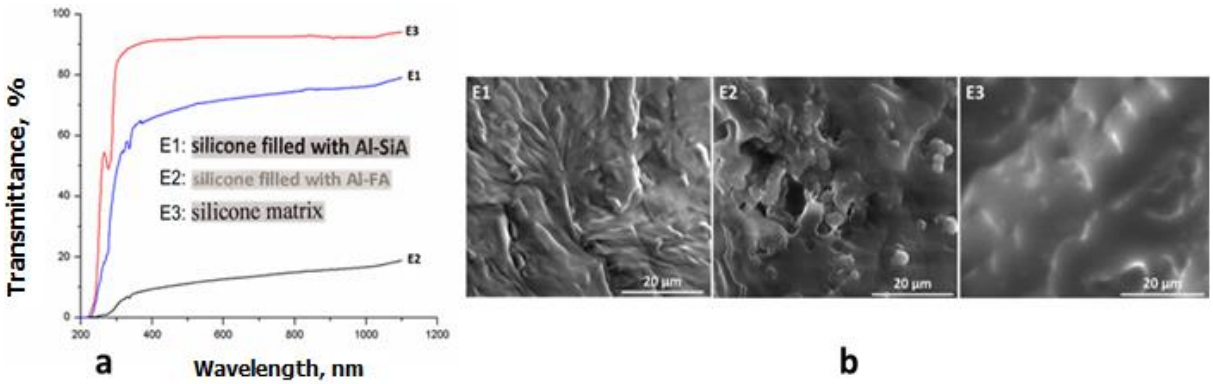

Figure 6.11.a. UV-Vis transmittance curves for silicone films with incorporated filler materials: **E1** – 10 wt% AlSiA; **E2** – 10 wt% AlFA; **E3** – neat silicone (film thickness: **E1** – 0.261 mm, **E2** – 0.196 mm, **E3** – 0.183 mm). Insert: Comparative photos illustrating the transparency of the silicone films. **b.** SEM image of the cross-section of film **E1** compared with the corresponding images of films **E2** and **E3** (reference film).

The UV-Vis transmittance spectra (Figure 6.11a) indicate that incorporating 10 wt% ***AlSiA*** reduces the film's transparency at 600 nm by 22.3% compared to a control film prepared under similar conditions but without filler material. This decrease is significantly smaller (almost four times less) than in the case of the film containing aluminum fumarate, prepared under similar conditions, where transparency drops by 86.3% compared to the neat silicone matrix. This highlights the good dispersion and compatibility of the filler material with the polymer matrix, a fact also supported by the *SEM* images (Figure 6.11b).

Remarkable results were also observed in the mechanical properties of the silicone film with ***AlSiA***. It can be seen that by adding only 10 wt% ***AlSiA***, both the modulus and elongation at break increase to 4.14 MPa and 1080%, respectively, compared to 0.78 MPa and 350% for the reference film **E3,** or compared to 1.76 MPa and 770% for film **E2** filled with the ***AlFA*** complex (Table 6.3).

Table 6.3. Main mechanical parameters determined from the stress–strain curves

Sample	Elongation at Break, Sm (%)	Nominal Stress at Break, Tnm (MPa)	Young's Modulus at 10% Elongation, Y (MPa)
E1	1080	2.50	4.14
E2	770	1.76	1.74
E3	350	0.78	0.33
E1 (10 wt% AlSiA), **E2** (10 wt% AlFA), **E3** (no filler).			

Such performance, consisting of significant simultaneous increases in both modulus and elongation, can be explained by the good dispersion of the filler and the interfacial interaction between the filler and the polymer chain. Therefore, ***AlSiA*** can be a promising solution for obtaining a transparent and highly elastic silicone material with high mechanical strength.

CHAPTER 7. MANGANESE COMPLEXATION WITH SILANE-DICARBOXYLIC ACID

7.2. Synthesis of the manganese complex

Mn(NO3)2×4H2O was treated with bis(p-carboxyphenyl)diphenylsilane (H2L), DPCS, an acid synthesized in the laboratory, in a 3:1 molar ratio in DMSO under solvothermal conditions to obtain the corresponding coordination compound (Scheme 7.1).

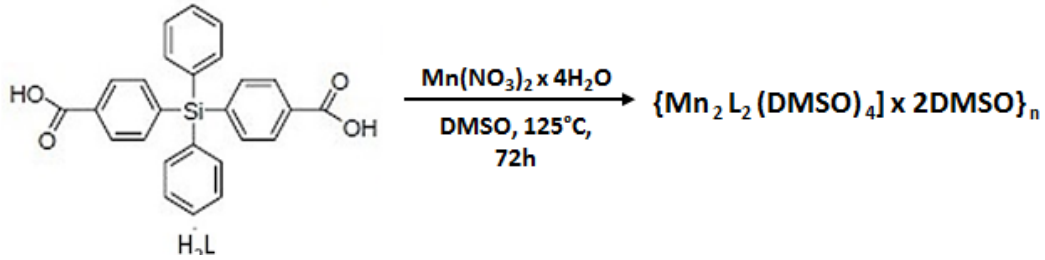

Scheme 7.1. Representation of the coordination reaction between ***Mn(II)*** and ***bis(p-carboxyphenyl)diphenylsilane (H2L)***

7.3. Structural characterization of the manganese complex

7.3.1. Fourier transform infrared spectroscopy (FTIR)

For the obtained compound, characteristic absorption bands of the carboxyl groups, υ_as(COO) and υ_s(COO^-), were identified at 1590 and 1428 cm^{-1} respectively, indicating a bidentate coordination mode of the carboxyl groups to Mn(II) (Figure 7.1). In addition to these bands, a band at 1644 cm^{-1} assigned to υ_as(COO^-) appears, suggesting that monodentate coordination of carboxyl groups is also present in the obtained compound. Structural analysis confirmed that both coordination modes exist in the isolated product: *monodentate* (Δ = 216 cm^{-1} > Δ of sodium salt) and *bridging bidentate* (Δ = 162 cm^{-1} < Δ of sodium salt). The band at 1662 cm^{-1} in the 1700–1500 cm^{-1} spectral region is attributed to the C=O vibration of water molecules bound within the compound's structure (Figure 7.1a). The newly formed Mn-O bonds are highlighted by the band at 554 cm^{-1} (Nakamoto, 1986).

7.3.2. Crystallographic analysis

The crystallographic analysis revealed that the structure of the formed complex, Mn_2L_2, features a dinuclear node consisting of two manganese atoms bridged by two carboxylate groups in a syn-syn bidentate bridging mode, along with a water molecule coordinated in a μ-aqua-bridging fashion.

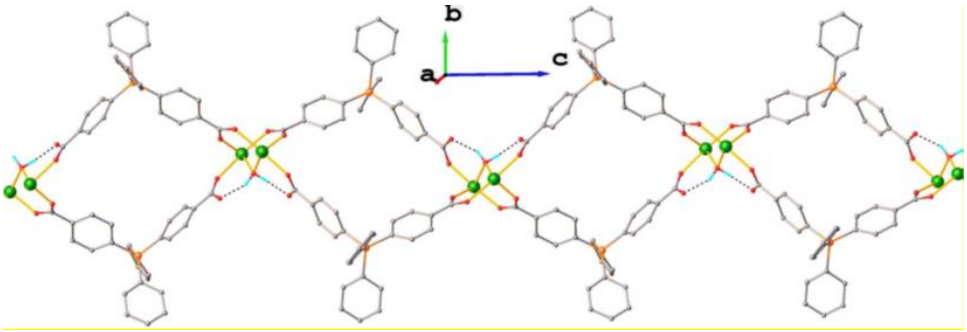

Figure 7.3. The structure of the 1D coordination polymer in the crystal structure.

A one-dimensional (1D) coordination polymer is formed, and the largest spherical void resulting from the packing of the coordination polymer in the crystal does not exceed 17.2 Å³ (Figure 7.3).

7.4. Study of the properties of the manganese complex

7.4.1. Photophysical properties

The photophysical properties of ligand L and the synthesized Mn_2L_2 complex were investigated both in solution (in DMF) and in the solid state using electronic absorption and emission spectroscopy. The UV-Vis absorption spectrum of ligand L (Figure 7.5), recorded in DMF solution, shows very weak peaks at 280 nm (ε = 5378 L/mol·cm), 288 nm (ε = 4176 L/mol·cm), and 308 nm (ε = 553 L/mol·cm), which are attributed to π-π* and σ-σ* transitions in the tetraphenylsilane unit. Upon coordination, a bathochromic shift occurs, with the 308 nm band shifting to 360 nm, accompanied by a decrease in intensity and broadening, forming a broad band attributed to ligand-to-metal charge transfer (LMCT).

The intense fluorescence of the ligand, visible by the emission maximum at 340 nm upon excitation at either 288 or 310 nm (Figure 7.5a), results from excitation of the tetraphenylsilane fragment. The fluorescence spectrum of the $\boldsymbol{Mn_2L_2}$ complex consists of two maxima, at 370 and 402 nm. These violet-blue emissions originate from charge transfer between the ligand and the metal. The fluorescence spectra of the ligand and the synthesized complex in crystalline state

(Figure 7.5b) are similar to those observed in solution, and are likewise centered on the ligand. The red shift of the emission peak in the complex is due to coordination of ligand L to the metal center.

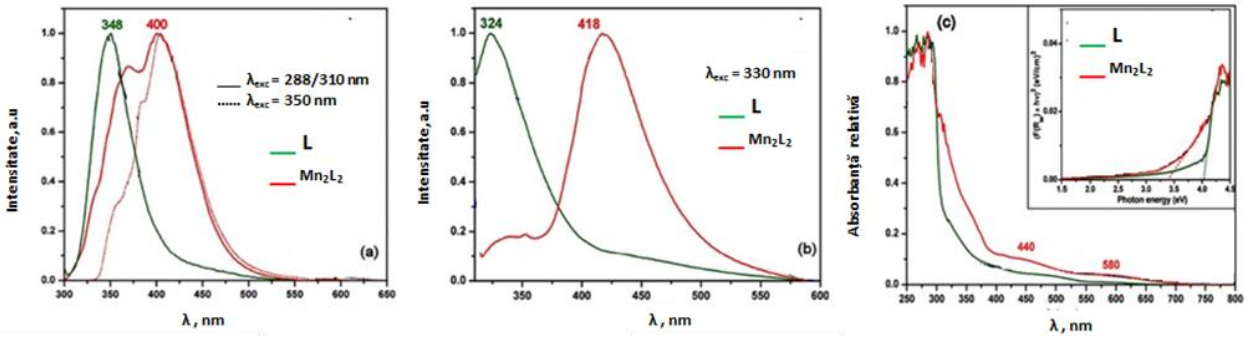

Figure 7.5. Normalized fluorescence spectra of the ligand H_2L (DPCS) and the Mn_2L_2 complex in: **(a)** DMF solution (c = 1.12 × 10^{-4} M/L); **(b)** solid state; **(c)** normalized diffuse reflectance spectra (DRS) of the ligand DPCS and the Mn_2L_2 complex; ***Inset***: plot of $[F(R\infty) \times h\nu]^2$ versus photon energy.

CHAPTER 9. GENERAL CONCLUSIONS

Based on literature studies, the potential for diversification of organosilicon compounds and enhancement of their performance through promising yet insufficiently explored pathways has been identified. Thus, a series of new compounds were synthesized by chemically modifying siloxane or silane precursors with organic functional groups, while optimizing the experimental protocols for synthesis, separation, and characterization. These compounds were analyzed in terms of their structure and properties (thermal, optical, dielectric, surface characteristics, humidity and nitrogen sorption, etc.).

For some of the obtained compounds, their application potential was investigated in fields such as antimicrobial agents, catalysts, dielectric materials, and electrolytes. However, the majority of the functionalized compounds obtained were approached—either through theoretical or experimental studies—from the perspective of their use as ligands in metal coordination chemistry. As with the ligands, the resulting complexes were characterized structurally, in terms of properties, and, in some cases, their applications were also explored.

The personal contributions consist of the synthesis and characterization of **22 new compounds** (eight of which are registered in the **CCDC** database), as well as **one material** (a

silicone elastomer reinforced with a MOF based on siloxane-dicarboxylic acid and aluminum ions). These were synthesized/prepared and studied as follows:

- ***Six new compounds*** were obtained by the chemical modification of *bis(chloroalkyl)-substituted silanes/siloxanes* with three differently substituted *mercaptotriazole derivatives*, one of which was also synthesized during this doctoral research. The compounds resulting from the **thiol-alkylation reaction** were characterized by elemental, spectral, and crystallographic analyses, and their structures were registered in the CCDC crystallographic database**.** Their thermal behavior**,** antimicrobial activity, and *hydrophilic-lipophilic balance (HLB)* were evaluated. Regarding their metal ion binding capacity, among the investigated metal ions (Cu^{2+}, Zn^{2+}, Mn^{2+}, Co^{2+}, and Ni^{2+}), these ligands showed a clear selectivity toward Cu^{2+} ions, indicating strong potential for metal ion sensing applications.

- ***Nine siloxane derivatives functionalized with carboxyl/thioacetyl groups*** were obtained through **thiol-ene addition** (photoactivated or thermally activated in the presence of suitable catalysts) of three thiol derivatives: *3-mercaptopropionic acid**,** thioglycolic acid*, and *thioacetic acid*. The resulting products were structurally characterized by spectral analysis (FTIR and NMR)**.** The modification degree of vinyl groups in the carboxyl-functionalized silicone precursors, evaluated from ^{1}H NMR spectra**,** ranged between 69 and 86 mol%**.** These compounds exhibited self-assembly behavior in solution, as demonstrated by DLS and NTA analyses. This behavior was also supported by calculated HLB values ranging from 8.9 to 10.94, placing them at the border between wetting/dispersing agents and oil/water emulsifiers. A correlation was identified between the calculated dipole moment values, measured glass transition temperatures, and HLB values. The compounds showed higher permittivity and conductivity values, which were significantly amplified by lithium ion doping, compared to the original vinylsiloxane precursors.

- ***Three copper complexes of carboxyl-functionalized cyclosiloxanes*** were synthesized, differing in the size of the siloxane ring (cyclotri- or cyclotetrasiloxane) and the length of the spacer linking the carboxyl groups to the silicon atoms. The structures of the complexes were elucidated using combined techniques, including spectral methods (*IR, UV-Vis in diffuse reflectance mode), EDX*, and *PXRD*. These complexes exhibit a spherical morphology, facilitated by the self-assembly of the ligands in solution prior to coordination. They were shown

to possess antifungal and catalytic activity. Calcination of the complexes leads to structured materials containing silicon and copper in a ratio similar to that in the original compounds.

• ***A dicarboxylic acid with a tetramethyldisiloxane spacer (1,3-bis(carboxypropyl)-tetramethyldisiloxane)*** was isolated and characterized for the first time by crystallographic analysis. Based on this acid, an aluminum complex was obtained, apparently isostructural with the commercial analog based on adipic acid and aluminum, but characterized by dense packing with a specific surface area of 28.15 m^2/g, attributed to the flexibility of the *tetramethyldisiloxane* spacer. This compound proved to be an effective reinforcing agent for silicone elastomers.

• ***A new silicone composite*** was developed, based on a silicone matrix incorporating the aluminum complex and the dicarboxylic acid with a siloxane spacer. The composite elastomer demonstrated good transparency and superior mechanical properties compared to a similar silicone without any additive.

• ***A one-dimensional coordination polymer***, based on a *dicarboxylic acid with a silane* spacer (*bis(p-carboxyphenyl)diphenylsilane*), previously obtained, and *Mn(II)* ions, was synthesized under solvothermal conditions. The structure of the isolated compound was determined by crystallographic analysis, complemented by spectral and elemental analysis. This compound exhibits violet-blue emission and shows potential for application in optoelectronic devices, particularly light-emitting devices.

PERSPECTIVES:

- Modification of the substituents on the silicon atoms and integration into advanced hybrid structures for fine-tuning of electronic, catalytic, optical, and other properties;
- Exploitation of the silicon-containing fragment in supramolecular chemistry to promote self-assembly and to generate structures useful in the design of nanostructured systems;
- Leveraging specific features such as the hydrophobicity and bulkiness of the silicon structural motif in the design of compounds with controlled biomolecular interactions;

- A more intensive approach to computational chemistry for the design of organosilicon compounds and the prediction of their chemical behavior in complex systems.

These perspectives further highlight the fact that the silicon-containing structural fragment holds significant, yet still underexplored, potential. Organosilicon materials continue to offer remarkable opportunities for the development of innovative functional structures with applications across diverse fields.

SCIENTIFIC ACTIVITY

The original results presented in this thesis have been published as scientific articles in indexed international and national ISI journals.

ISI ARTICLES PUBLISHED WITHIN THE THESIS:

1. **Turcan-Trofin G.O.**, Zaltariov M.F., Roman G., Shova S., Vornicu N., Balan-Porcarasu M., Isac D.L., Neamtu A., Cazacu M. **(2019)** *Amphiphilic silicone-bridged bis-triazoles as effective, selective metal ligands and biologically active agents in lipophilic environment*. Journal of Molecular Liquids, 111560. https://doi.org/10.1016/j.molliq.2019.111560, WOS: 000506712400005 (F.I.=5,3; Q1)

2. **Turcan-Trofin G.O**., Zaltariov M.F., Iacob M., Tiron V., Branza F., Racles C., Cazacu M. **(2019)** *Copper(II) complexes with spherical morphology generated in one step by amphiphilic ligands: in situ view of the self-assembling, characterization, catalytic activity*. Colloids and Surfaces A-Physicochemical and Engineering Aspects, 123756. https://doi.org/10.1016/j.colsurfa.2019.123756, WOS: 000488954800058 (F.I.=4,9; Q2)

3. **Turcan-Trofin GO**; Asandulesa M., Balan-Porcarasu M., Varganici C.D., Tiron V., Racles C., Cazacu M. **(2019)** *Linear and cyclic siloxanes functionalized with polar groups by thiol-ene addition: Synthesis, characterization and exploring some material behavior*. Journal of Molecular Liquids, 282, 187-196. https://doi.org/10.1016/j.molliq.2019.03.005, WOS:000465060400021 (F.I.=5,3; Q1)

4. Cazacu M., **Turcan-Trofin G.O**., Vlad A., Bele A., Shova S., Nicolescu A., Bargan A. **(2019)** *Hydrophobic, amorphous metal-organic network readily prepared by complexing the aluminum ion with a siloxane spaced dicarboxylic acid in aqueous medium*. Journal of Applied Polymer Science , 47144. doi:10.1002/app.47144, WOS:000454228400035 (F.I.=2,7; Q2)

5. Turcan-Trofin G.O., Avadanei M., Shova S., Vlad A., Cazacu M., Zaltariov M.F. **(2018)** *Metallo-supramolecular assemblies of dinuclear Zn(II) and Mn(II) secondary building units (SBUs) and a bent silicon dicarboxylate ligand.* Inorganica Chimica Acta, 483, 454-463, https://doi.org/10.1002/app.47144, WOS:000445543100058 (F.I.=2,7; Q2)

6. Cazacu M., Damoc M., Dascalu M., **Turcan-Trofin G.-O.** (**2025**) Permethylated silicon: a structural motif with a critical role in shaping the properties of organic-inorganic compounds" Journal of Inorganic and Organometallic Polymers and Materials – *acceptată* (F.I.=3,9; Q2)

CONFERENCES:

1. **Turcan-Trofin G.-O**., Roman G., Vornicu N., Shova S. Cazacu M. *Siloxani funcționalizați cu heterocicluri cu azot*. Zilele Academice Ieșene (ZAI), Iași, România, 2017.

2. **Turcan-Trofin G.-O**., Roman G., Vornicu N., Shova S., Cazacu M. *New silicone derivatives with biocidal activity, Current Trends in Bionanotechnologies,* A XXVIII-a ediție a Congresului Internațional sub sloganul „Pregătim viitorul promovând excelența", Apollonia, Iasi, România, 1-4 martie 2018.

3. **Turcan-Trofin G.-O.**, Zaltariov M.-F., Shova S. Cazacu M. *New ligands and materials developed on silicone substrates.* Tenth Cristofor I. Simionescu Symposium: Frontiers in Macromolecular and Supramolecular Science (CIS), București, România, 11-14 iunie 2018.

4. Zaltariov M.-F., **Turcan-Trofin G.-O**., Shova S., Racles C. Cazacu M. *Versatility of Silane/Siloxane Building Blocks in Coordination Driven Self-assembling*. Tenth Cristofor I. Simionescu Symposium: Frontiers in Macromolecular and Supramolecular Science, (CIS), Academia Română, București, 8–14 iunie 2018. (*Invited conference*)

POSTERS:

1. **Turcan-Trofin G.-O**., Zaltariov M.-F., Tugui C., Cazacu M. *Copper coordination compounds with spherical morphology based on methylcyclosiloxanes functionalized with carboxyl groups as ligands.* 12th International Conference on Physics of Advanced Materials (ICPAM-12), Creta, Grecia. 22-28 septembrie 2018.

2. **Turcan-Trofin G.-O**., Zaltariov M.-F., Shova S., Cazacu M. et al., *Functionalization of siloxane derivatives by attaching polar groups.* 21st International Conference on Solid Compounds of Transition Elements (SCTE 2018), Viena, Austria, 25-29 martie 2018.

3. Zaltariov M.-F., Avădanei M., **Turcan-Trofin G.-O.**, Vlad A., Cazacu M. Shova, S. *Lanthanide-based MOFs built on silicon-containing carboxylate ligands: Synthetic strategies and properties evaluation.* 21st International Conference on Solid Compounds of Transition Elements (SCTE 2018), Viena, Austria, 25-29 martie 2018.

4. Cazacu M., **Turcan-Trofin G.-O**., Zaltariov M.-F., Dascalu M., Vornicu N. Shova S. *Bis-triazoles spaced by a dimethylsilane or tetramethyldisiloxane motif as new ligands and biologically active agents*, 21st Romanian International Conference on Chemistry and Chemical Engineering (RICCCE'21), S6, Constanța-Mamaia, România, 4-7 septembrie 2019.

OTHER SCIENTIFIC ACTIVITIES:

1. *3rd Training School organizat de COST* Action CA15119 (NANOUPTAKE); Rzeszow (Poland); 19-21 Septembrie 2018.

RESEARCH PROJECTS:

1. Rețele metal-organice cu hidrofobicitate fin controlată utilizând chimia siliconilor (SiMOFs), Contract 114/2017/ Director proiect: Dr. Maria Cazacu
2. Mimarea mecanismelor viului prin abordări ale chimiei supramoleculare, în cinci dimensiuni (5D-nanoP), PN-III-P4-ID-PCCF-2016-0050, Contract 4/2018/ Director proiect: Prof. Aatto Laaksonen; Responsabil partener: Dr. Maria Cazacu

SELECTED BIBLIOGRAPHY

Alvarez, E., Guillou, N., Martineau, C., Bueken, B., Van De Voorde, B., Guillouzer, C.L., Fabry, P., Nouar, F., Taulelle, F., De Vos, D., Chang, J., Cho, K.H., Ramsahye, N., Devic, T., Daturi, M., Maurin, G. and Serre, C. (2015). The structure of the aluminum fumarate metal–organic framework A520. *Angewandte Chemie International Edition*, 54(12), 3664–3668. https://doi.org/10.1002/anie.201410459

Ayati, A., Emami, S. and Foroumadi, A. (2016). The importance of triazole scaffold in the development of anticonvulsant agents. *European Journal of Medicinal Chemistry*, 109, 380-392. https://doi.org/10.1016/j.ejmech.2016.01.009

Brown, D.G. (1993). *Effects of metal catalysed peroxide decomposition on the bleaching of mechanical pulp.* University of Tasmania. Thesis. https://doi.org/10.25959/23236583.v1

Bruce, D.W., O'Hare, D. and Walton, R.I. (2011) *Energy materials*. Wiley. Chapter 4, 245-272. ISBN:9780470997529

Cao, Q. and Che, R. (2014) Synthesis of near-infrared fluorescent, elongated ring-like Ag2Se colloidal nanoassemblies. *RSC Advances*, 4(32), 16641. https://doi.org/10.1039/c4ra00613e

Davies, J.T. (1957). A quantitative kinetic theory of emulsion type, I. physical chemistry of the emulsifying agent. Gas/liquid and liquid/liquid interface; *Proceedings of the International Congress of Surface Activity*, 426–438.

Georén, P. and Lindbergh, G. (2003). On the use of voltammetric methods to determine electrochemical stability limits for lithium battery electrolytes. *Journal of Power Sources*, 124(1), 213–220. https://doi.org/10.1016/s0378-7753(03)00739-0

Goldstein, J. (1974). The kinetics of hydrogen peroxide decomposition catalyzed by cobalt-iron oxides. *Journal of Catalysis*, 32(3), 452–465. https://doi.org/10.1016/0021-9517(74)90096-7

Griffin, W.C. (1949). Classification of surface-active agents by 'HLB'. *Journal of the Society of Cosmetic Chemists*, (5), 311–326.

Griffin, W.C. (1954). Calculation of HLB values of non-ionic surfactants. *Journal of the Society of Cosmetic Chemists*, 5(4), 249–256.

Irving, H., Williams, R.J.P. (1953). The stability of transition-metal complexes. *Journal of the Chemical Society (Resumed)*, 3192. https://doi.org/10.1039/jr9530003192

Krüger, M., Inge, A.K., Reinsch, H., Li,Y., Wahiduzzaman, M., Lin, C., Wang, S., Maurin, G., and Stock, N. (2017). Polymorphous AL-MOFs based on V-Shaped linker molecules: synthesis, properties, and in situ investigation of their crystallization. *Inorganic Chemistry*, 56(10), 5851–5862. https://doi.org/10.1021/acs.inorgchem.7b00202

Launer P.J. (1987). *In Silicone Compounds Register and Review*, ed. Arkles, B., Petrarch Systems.

Lee, H., Lee, H., Seo, J., Kim, H., Shin, Y.K., Kim, J. and Lee, C. (2016). Activation of oxygen and hydrogen peroxide by copper(II) coupled with hydroxylamine for oxidation of organic contaminants. *Environmental Science & Technology*, 50(15), 8231–8238. https://doi.org/10.1021/acs.est.6b02067

Nakamoto, K. (1986). *Infrared and Raman Spectra of Inorganic and Coordination Compounds*; Wiley: New York, USA 203 – 236 ISBN 978-0-471-74493-1, 1986.

Plech, T., Wujec, M., Kosikowka, U. and Malm, A. (2013). Synthesis and antibacterial activity of 4,5-disubstituted-1,2,4-triazole-3- thiones. *Letters in Drug Design & Discovery*,. https://doi.org/10.2174/15701808113109990082

Pretsch, E., Badertscher, M. and Bühlmann, P. (2009). *Structure determination of organic compounds*. Springer Berlin, Heidelberg, eBook ISBN 978-3-540-93810-1. https://doi.org/10.1007/978-3-540-93810-1

Racles, C., Dascalu, M., Bele, A., Tiron, V., Asandulesa, M., Tugui, C., Vasiliu, A. and Cazacu, M. (2017). All-silicone elastic composites with counter-intuitive piezoelectric response, designed for electromechanical applications. *Journal of Materials Chemistry C*, 5(28), 6997–7010. https://doi.org/10.1039/c7tc02201h

Racles, C., Zaltariov, M., Iacob, M., Silion, M., Avadanei, M. and Bargan, A. (2016). Siloxane-based metal–organic frameworks with remarkable catalytic activity in mild environmental photodegradation of azo dyes. *Applied Catalysis B Environment and Energy*, 205, 78–92. https://doi.org/10.1016/j.apcatb.2016.12.034

Skounas, S., Methenitis, C., Pneumatikakis, G. and Morcellet, M. (2010). Kinetic studies and mechanism of hydrogen peroxide catalytic decomposition by Cu(II) complexes with polyelectrolytes derived from l-alanine and glycylglycine. *Bioinorganic Chemistry and Applications*, 2010(1). https://doi.org/10.1155/2010/643120

Stock, N. (2014). Metal-Organic frameworks: aluminium-based frameworks. *Encyclopedia of Inorganic and Bioinorganic Chemistry*, 1–16. https://doi.org/10.1002/9781119951438.eibc2197

Zhang, Z., Lyons, L.J., Jin, J.J., Amine, K. and West, R. (2005). Synthesis and Ionic Conductivity of Cyclosiloxanes with Ethyleneoxy-Containing Substituents. *Chemistry of Materials*, 17(23), 5646–5650. https://doi.org/10.1021/cm050742x